Optimization of Reaction Rate Parameters in Modeling of Heavy Paraffins Dehydrogenation

Leila Vafajoo, Farhad Khorasheh, Mehrnoosh Hamzezadeh Nakhjavani and Moslem Fattahi

Abstract—In the present study, a procedure was developed to determine the optimum reaction rate constants in generalized Arrhenius form and optimized through the Nelder-Mead method. For this purpose, a comprehensive mathematical model of a fixed bed reactor for dehydrogenation of heavy paraffins over Pt–Sn/Al$_2$O$_3$ catalyst was developed. Utilizing appropriate kinetic rate expressions for the main dehydrogenation reaction as well as side reactions and catalyst deactivation, a detailed model for the radial flow reactor was obtained. The reactor model composed of a set of partial differential equations (PDE), ordinary differential equations (ODE) as well as algebraic equations all of which were solved numerically to determine variations in components' concentrations in term of mole percents as a function of time and reactor radius. It was demonstrated that most significant variations observed at the entrance of the bed and the initial olefin production obtained was rather high. The aforementioned method utilized a direct-search optimization algorithm along with the numerical solution of the governing differential equations. The usefulness and validity of the method was demonstrated by comparing the predicted values of the kinetic constants using the proposed method with a series of experimental values reported in the literature for different systems.

Keywords—Dehydrogenation, Pt-Sn/Al$_2$O$_3$ Catalyst, Modeling, Nelder-Mead, Optimization

I. INTRODUCTION

THE dehydrogenation of paraffins is an important reaction in the synthesis of monomers for synthetic rubber and other products. During the World War II, catalytic dehydrogenation of butanes over a chromia-alumina catalyst was practiced for butanes production, which were then dimerized to octane and hydrogenated to yield high-octane aviation fuel. Platinum catalysts usually supported on aluminum oxide [1-3] exhibited a high efficiency in the dehydrogenation of paraffins to olefins. Promoters improved the activity, selectivity, and stability of platinum-alumina catalysts. The most frequent side reaction led to catalyst

L. Vafajoo is with the Chemical and Environmental Engineering Faculty, Fannie College, Islamic Azad University, South Tehran Branch, Ahang Blvd., P.O. Box 1777613651, Tehran, I.R. Iran (corresponding author; phone: +98-21-3301-0400; fax: +98-21-3371-7140; e-mail: vafajoo@azad.ac.ir).

F. Khorasheh is with Department of Chemical and Petroleum Engineering, Sharif University of Technology, Azadi Avenue, P.O. Box 11365-9465, Tehran, Iran (e-mail: khorashe@sharif.edu)

M.H. Nakhjavani is with the Chemical and Environmental Engineering Faculty, Fannie College, Islamic Azad University, South Tehran Branch, Ahang Blvd., P.O. Box 1777613651, Tehran, I.R. Iran

M. Fattahi is with the Department of Chemical and Petroleum Engineering, Sharif University of Technology, Azadi Avenue, P.O. Box 11365-9465, Tehran, Iran (e-mail: moslemfattahi@che.sharif.edu)

deactivation was the formation of coke. The preliminary sulfiding of catalysts is used to reduce coke formation [4, 5]. Sulfiding somewhat decreased the catalyst activity but significantly increased their stability [6-8]. Selective dehydrogenation of higher paraffins (C$_{10}$-C$_{14}$) to the corresponding mono olefins on the promoted Pt/Alumina catalyst is an industrially important process and a key step in the manufacture of bio-degradable detergents. The reaction was carried out in a radial flow fixed bed reactor at high temperatures (723-773 K) and low pressures (200-300 kPa), with hydrogen as diluent. Small amounts of di-olefins and aromatics were formed by subsequent secondary dehydrogenation reactions. All these products led to the formation of light paraffins by cracking. Studies on kinetics usually help to develop the reaction mechanism, hence establish reaction network of a process. Therefore, it is a necessary tool for simulation and design of commercial reactors. The kinetics studies also help to evaluate catalyst efficiency and attempted improvements thereof [9]. The main reaction in catalytic dehydrogenation is the formation of mono-olefins from the corresponding feed paraffin. Other reactions include consecutive and side reactions. The reaction pathways involved in heavy paraffin dehydrogenation (*e.g.*; detergent-range C$_{10}$-C$_{14}$ *n*-paraffins) were more complicated than those in light paraffin dehydrogenation (*e.g.*, propane and isobutane). The main difference in reaction pathways was that a significant amount of cyclic compounds might have been formed via dehydrocyclization from heavy paraffins which was not the case for light paraffins. The consecutive reactions as well as; the dehydrogenation of mono-olefins to diolefins and triolefins, were catalyzed on the same active sites as the dehydrogenation of paraffins to mono-olefins. The consecutive reactions formed triolefins, aromatics, dimers, and polymers must have been suppressed kinetically or by catalyst modifications [10,11]. The heart of a Paraffin dehydrogenation plant is its reactor. Several routes have been utilized for the production of linear alkylbenzene [11]. Databases providing measurements of reaction rate parameters for various reactions are available in the literature. These gave data in terms of the logarithm of the reaction rate as a function of 1/T in which a large variation of the reaction rate at all temperatures were generally observed. Furthermore, the effect of temperature increases might translate into either an increase or decrease of the reaction rate, depending on which set of data was taken to be the more accurate. Since there is so much uncertainty in the rate data, problems occur when calculating species concentration for the products [12]. The determination of the optimal reaction rate parameters for a given reaction

mechanism is a complex task as it involves parameter estimation procedures for a dynamical model stated in a form of differential equations [13]. Various traditional gradient based algorithms might be applied to the optimization of chemical systems and various technique employed in order to adapt the standard algorithms to the chemical kinetics problem considered [14-16]. However, a major drawback of all gradient based methods is the fact that they only converge to the next local optimum of the objective functions. For objective functions with complex, highly structured landscape, such as those encountered in chemical kinetics modeling, this is clearly unsatisfactory. The results are affected by the accuracy of the initial guess and often, in practice, an initial guess which is close to the true solution of the problem might not be constructed. Moreover, for large chemical systems, with large numbers of variables, the gradient computations are difficult to be performed accurately, in particular since the matrices involved may be ill-conditioned. From this perspective, stochastic methods appear to be more promising due to their ability to cope with uncertainty, insufficient information and noisy data.In this research, a thorough modeling of a heavy paraffin dehydrogenation reactor was carried out utilizing actual data from a commercial plant, however, accurate data for the rate constants of different chemical steps in the reaction mechanism were still lacking. Authors attempted to optimize the reaction rate data utilizing Nelder-Mead (NM) method to predict the reaction rate parameters for possible reactions presented.

II. NELDER-MEAD SIMPLEX METHOD

The name direct search referred to the fact that the search for the optimum is carried out directly without the help of a process model. This further implied that the direct approach needed less measurement data since data required to build and update process models become unnecessary. Thus, as a reminder, the direct search method is recommended when the process has one or more of the following properties [17]:
1. Process model is difficult or expensive to obtain.
2. Process exhibits discontinuities.
3. Measurement of the process data is expensive or time-consuming or
4. The measurement data are contaminated by significant noise.
The NM simplex method is a very efficient local search procedure but its convergence is extremely sensitive to the selected starting point which is a local search method designed for unconstrained optimization without using gradient information [18-22]. The NM modified to handle constrained optimization and the aforementioned steps are described in literature [23, 24].

III. MODELING

A. Reaction rate parameters

The net chemical production rate of each species resulted from a competition between all the chemical reactions involving that species. It was assumed that each reaction proceeds according to the law of mass action and the rate coefficients were of modified Arrhenius form, *i.e.:*
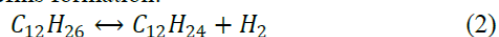
$$K_i = A_i T^{\beta_i} \exp\left(-\frac{E_i}{RT}\right) \tag{1}$$

The rate constant equations (1) contain three parameters A_i, β_i and E_i for the ith reaction. It is possible to determine these parameters for each reaction based upon outlet experimental mole fractions alone; which is the subject focused upon in this paper. Accordingly, the β_i assigned zero and the Arrhenius form of K_i with two parameters of A_i and E_i optimized through the Nelder-Mead method.
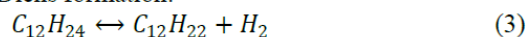
B. The kinetic model

Padmavathi *et al.* studied the kinetics of n-dodecane dehydrogenation over a Pt–Sn/Al$_2$O$_3$ catalyst between 733 and 763K and derived the reaction kinetics scheme based upon Langmuir-Hinshelwood-Hougen-Watson (LHHW) mechanistic model [9]. In their study they considered the product distribution and their observations showed that the system might have been described by the following reactions:
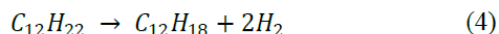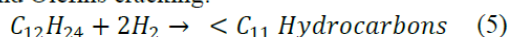
Olefins formation:
$$C_{12}H_{26} \longleftrightarrow C_{12}H_{24} + H_2 \tag{2}$$
Diens formation:
$$C_{12}H_{24} \longleftrightarrow C_{12}H_{22} + H_2 \tag{3}$$
Aromatics formation:
$$C_{12}H_{22} \rightarrow C_{12}H_{18} + 2H_2 \tag{4}$$
And Olefins cracking:
$$C_{12}H_{24} + 2H_2 \rightarrow \ < C_{11} \ Hydrocarbons \tag{5}$$

rates of formation reactions for each component [9] might be expressed as:

$$r_1 = \frac{k_1 K_P(p_P - p_O p_H/K_{E1})}{(1 + K_P p_P + K_O p_O + K_D p_D + K_A p_A + K_H p_H)^2} \tag{6}$$

$$r_2 = \frac{k_2 K_O(p_O - p_D p_H/K_{E2})}{(1 + K_P p_P + K_O p_O + K_D p_D + K_A p_A + K_H p_H)^2} \tag{7}$$

$$r_3 = \frac{k_3 K_D p_D}{(1 + K_P p_P + K_O p_O + K_D p_D + K_A p_A + K_H p_H)^2} \tag{8}$$

$$r_4 = k_4 p_O \tag{9}$$

The values of the kinetic parameters along with standard error of kinetic coefficients presented in Ref. [9].

C. The mathematical model

A mathematical model based upon the above reaction was assumed. This model consisted of mass balances on the species present in the reactor led to a series of algebraic and differential equations [25, 26]. The pseudo homogenous model consisted of material balances for different species resulting in a number of differential equations in radial coordinate where the diffusion term was assumed negligible compared with the bulk flow. Because of gas radial flow, velocity change and pressure drop occurred in radial coordinate [27]. In addition, the momentum balance was written as Bernoulli's equation [26]:

$$\frac{dP}{\rho} + d\left(\frac{u^2}{2}\right) + dh_{fs} = 0 \qquad (10)$$

$$dh_{fs} = f \frac{u^2}{2} \frac{dr}{R_H} \qquad (11)$$

$$f = \frac{(1-\varepsilon)^2}{\varepsilon^3} \frac{75}{(D_P \rho u/\mu)} \qquad (12)$$

$$R_H = \frac{cross\ section\ available\ for\ flow}{wetted\ perimeter} = \frac{\varepsilon}{a} \qquad (13)$$

$$a = (1-\varepsilon)\frac{6}{D_P} \qquad (14)$$

Pressure in this equation was calculated through the Peng-Robinson equation of state [28]. Furthermore, the continuity equation (15) simplified to the equation (16) for a constant density system.

$$\frac{\partial \rho}{\partial t} + u\nabla \rho = -\rho(\nabla u) \qquad (15)$$

$$\frac{\partial \rho}{\partial r} = -\frac{\rho}{u}\frac{\partial u}{\partial r} - \frac{\rho}{r} \qquad (16)$$

Based upon aforementioned assumptions, governing differential equations were determined to be [29]:

$$\frac{\partial C_P}{\partial t} = \frac{C_P u}{r\varepsilon} + \frac{u}{\varepsilon}\frac{\partial C_P}{\partial r} + \frac{C_P}{\varepsilon}\frac{\partial u}{\partial r} + d_{load}\,a_c(-r_1) \qquad (17)$$

This last relationship may be rewritten for each reaction component.
Furthermore, molar balance for the olefin is as follows:

$$\frac{\partial C_O}{\partial t} = \frac{C_O u}{r\varepsilon} + \frac{u}{\varepsilon}\frac{\partial C_O}{\partial r} + \frac{C_O}{\varepsilon}\frac{\partial u}{\partial r} + d_{load}a_c(r_1 - r_2 - r_4) \qquad (18)$$

And, the molar balance for diene species is as follows:

$$\frac{\partial C_D}{\partial t} = \frac{C_D u}{r\varepsilon} + \frac{u}{\varepsilon}\frac{\partial C_D}{\partial r} + \frac{C_D}{\varepsilon}\frac{\partial u}{\partial r} + d_{load}\,a_c(r_2 - r_3) \qquad (19)$$

Whereas, the molar balance for aromatics is given by:

$$\frac{\partial C_A}{\partial t} = \frac{C_A u}{r\varepsilon} + \frac{u}{\varepsilon}\frac{\partial C_A}{\partial r} + \frac{C_A}{\varepsilon}\frac{\partial u}{\partial r} + d_{load}\,a_c(r_3) \qquad (20)$$

Ultimately, the molar balance for light paraffins was provided by:

$$\frac{\partial C_{LP}}{\partial t} = \frac{C_{LP} u}{r\varepsilon} + \frac{u}{\varepsilon}\frac{\partial C_{LP}}{\partial r} + \frac{C_{LP}}{\varepsilon}\frac{\partial u}{\partial r} + d_{load}\,a_c(r_4) \qquad (21)$$

And, the molar balance for the hydrogen is presented by:

$$\frac{\partial C_H}{\partial t} = \frac{C_H u}{r\varepsilon} + \frac{u}{\varepsilon}\frac{\partial C_H}{\partial r} + \frac{C_H}{\varepsilon}\frac{\partial u}{\partial r} + d_{load}a_c(r_1 + r_2 + 2r_3 - 2r_4) \qquad (22)$$

The deactivation rate laws selected to be utilized in the current research was [3]:

$$t = \frac{1 - a_c^{(1-n-E_d/E_A)}}{k_{d0}(1 - n + E_d/E_A)} \qquad (23)$$

The feed flew inward in the radial direction from 0.75m at the inlet to a radius of 0.4m at the exit.
C_P, C_O, C_D, C_A, C_{LP} and C_H are density of paraffin, olefin, diene, aromatic, light paraffin and hydrogen; respectively. The d_{load} indicated the catalyst load density.

IV. NUMERICAL SOLUTION

The resulting partial differential equations (Equations (17)-(22)) were solved simultaneously utilizing the finite differences technique [30] subject to the initial and boundary

conditions. The discrete formulation of the equations was implicit and the three-point central formulae in the spatial domain and two-point forward difference formula for the time derivatives were employed. The PVT calculations were performed using the Peng-Robinson EOS. The kinetic coefficients in the reactions were optimized by Nelder-Mead optimization method and the results were compared with Ref. [9]. Optimized kinetic parameters resulted from the Nelder-Mead method used as a kinetic rate coefficient. Utilizing the experimental data from commercial plant, the 11 reaction rate constant functions (*i.e.*; 22 parameters) along with deactivation functions (*i.e.*; 4 parameters) were optimized. After obtaining optimizations with error of less than 1%, the rate constants were determined. The determined optimized parameters for kinetic rates and deactivation rate presented in Table 1. It should be noted that the CPU time consumption for programming was rather high which was also sensitive to the initial guesses; in addition, there was a possibility to get trapped in the relative minimum values.

TABLE I
OPTIMIZED KINETIC COEFFICIENT OF THE REACTIONS

$k_1 = 4.5046 \times 10^{15} \exp\left(\frac{-63.116}{RT}\right)$	$k_{-1} = 3.8788 \times 10^3 \exp\left(\frac{24.324}{RT}\right)$
$k_2 = 1.0473 \times 10^{15} \exp\left(\frac{-93.524}{RT}\right)$	$k_{-2} = 1.3773 \times 10^3 \exp\left(\frac{40.154}{RT}\right)$
$k_3 = 2.5909 \times 10^{16} \exp\left(\frac{-91.674}{RT}\right)$	$k_4 = 4.5063 \times 10^{14} \exp\left(\frac{-282.25}{RT}\right)$
$K_P = 2.2986 \times 10^2 \exp\left(\frac{18.996}{RT}\right)$	$K_O = 4.6224 \exp\left(\frac{74.980}{RT}\right)$
$K_H = 3.5614 \times 10^2 \exp\left(\frac{33.735}{RT}\right)$	$K_D = 6.4685 \exp\left(\frac{82.113}{RT}\right)$
$K_A = 6.3506 \exp\left(\frac{65.058}{RT}\right)$	
$n = 2.2194$	$E_d = 2.7469 \times 10^4$
$k_{d0} = 0.002178$	$E_A = 1.7766 \times 10^5$

V. RESULTS AND DISCUSSION

The investigated reactor was isothermal at 738.15 K. Figure 1 showed the variation of fluid superficial velocity across the reactor bed. The velocity and pressure profiles in the radial direction were obtained by solving equations (10) to (16) using the 4th order Runge-Kutta algorithm.
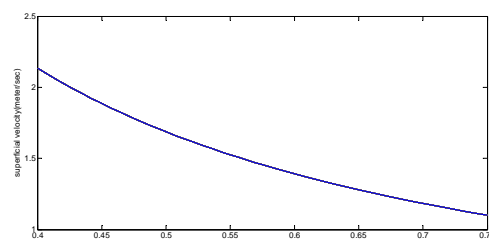

Fig. 1 The velocity profile for fixed bed reactor with radial feed flow

Results of simulation have been presented in Figures 2 to 7. Figure 2 illustrated variation of dynamic paraffin molar percent along the reactor. According to this Figure, paraffin molar percent increased with time. This is due to the catalyst deactivation which decreased paraffin conversion.
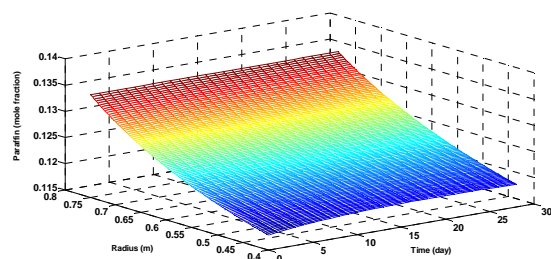
Fig. 2 Paraffin mole fraction as a function of time and reactor radius

Figure 3 illustrated the olefin mole fraction along the catalytic bed. It is seen that the Olefin percentage increased sharply along the catalytic bed at the reactor inlet reached a nearly constant value due to secondary side reactions involving the olefin. Furthermore, it is observed that the Olefin production lowered with time due to the catalyst deactivation.
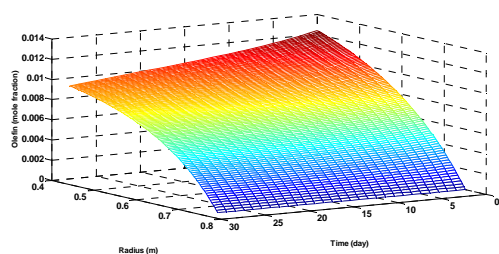

Fig. 3 Olefin mole fraction as a function of time and reactor radius

Figure 4 illustrated the dienes mole fraction as a function of bed radius. Similar trends as those for olefin production were observed for these materials as well.
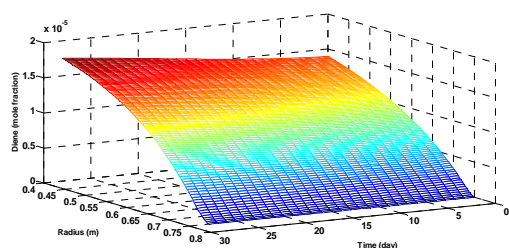

Fig. 4 Diene mole fraction as a function of time and reactor radius

Figure 5 indicated variations in the mole fraction of aromatics along the reactor bed which demonstrated a rational behavior of secondary products. In other words, aromatics formed from dienes which were primary reaction products.
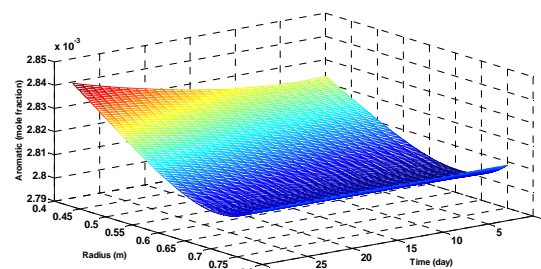

Fig. 5:Aromatic mole fraction as a function of time and reactor radius

Figure 6 depicted similar trends for light paraffins as were observed for aromatics generation. In other words, light paraffin production increased slowly. Figure 7 indicated a net increase in hydrogen along the reactor as it was produced via the reaction and only consumed through a side reaction. Furthermore, the species mole fraction presented in Table 2 suggested a good agreement between model estimations and industrial data existed.
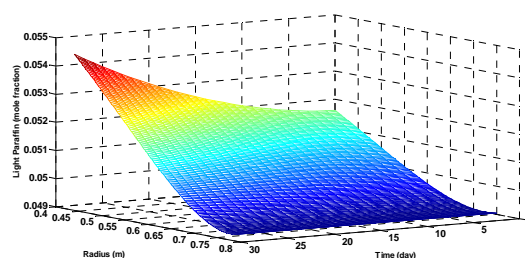

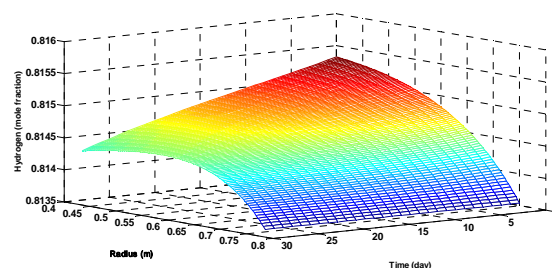Fig. 6 Light paraffin mole fraction as a function of time and reactor radius

Fig. 7 Hydrogen mole fraction as a function of time and reactor radius

TABLE II
THE NET SPECIES MOLE FRACTIONS PREDICTED BY MODEL THAT COMPARED BY INDUSTRIAL DATA

	Paraffin (mol) Exp.[29]	Paraffin (mol) Mod.	Olefin (mol) Exp.[29]	Olefin (mol) Mod.	Hydrogen (mol) Exp.[29]	Hydrogen (mol) Mod.
Start of run	0.1199	0.1178	0.0122	0.0124	0.8157	0.8153
After 10 days	0.1209	0.1192	0.0109	0.0110	0.8155	0.8150
After 16 days	0.1218	0.1193	0.0102	0.0104	0.8154	0.8148
After 22 days	0.1222	0.1194	0.0098	0.0098	0.8153	0.8146
After 28 days	0.1229	0.1195	0.0092	0.0092	0.8152	0.8143

VI. Conclusions

The Nelder-Mead optimization technique is a commonly used method in engineering using mathematical models or samples from experiments in real systems. In the present study, a dynamic reactor model was developed for dehydrogenation of heavy paraffins. The reaction kinetics and deactivation rate were optimized. The model was solved numerically to obtain variations of reaction products along the reactor bed. Variations of paraffin, olefin, diene, hydrogen and aromatics versus time and reactor radius investigated in this paper and their respective trends were determined. In spite of scares rate constant data for the process at hand, generated results of the present model all seemed logical and rational. The kinetic parameters of the reactions rate model have been optimized by Nelder-Mead method. The proposed kinetics coefficients were evaluated by the calculated result with the experimental data of commercial plant.

References

[1] George A. Olah, Hydrocarbon Chemistry, John Wiley, New York, 2002.
[2] N. A. Gaidai, S. L. Kiperman, Kinetic Models of Catalyst Deactivation in Paraffin Dehydrogenation, Kinetics and Catalysis 42 (2001) 527-532.
[3] Maryam Saeedizad, Saeed Sahebdelfar, Zahra Mansourpour, Deactivation kinetics of platinum-based catalysts in dehydrogenation of higher alkanes, Chemical Engineering Journal 154 (2009) 76-81.
[4] Victor K. Shum, John B. Butt, Wolfgang M. H. Sachtler, The effects of rhenium and sulfur on the activity maintenance and selectivity of platinum/alumina hydrocarbon conversion catalysts, Journal of Catalysis 96 (1985) 371-380.
[5] Robert W. Coughlin, Koei Kwakami, Akram Hasan, Activity, yield patterns, and coking behavior of Pt and PtRe catalysts during dehydrogenation of methylcyclohexane: I. In the absence of sulfur, Journal of Catalysis 88 (1984) 150-62.
[6] M. J. Dees, V. Ponec, On the influence of sulfur on the platinum/iridium bimetallic catalysts in n-hexane/hydrogen reactions, Journal of Catalysis 115 (1989) 347-355.
[7] J. Barbier, P. Marecol, Effect of presulfurization on the formation of coke on supported metal catalysts, Journal of Catalysis 102 (1986) 21-28.
[8] M.J. Dess, V. Ponec, The influence of sulfur and carbonaceous deposits on the selectivity and activity of Pt/Co catalysts in hydrocarbon reactions, Journal of Catalysis 119 (1990) 376-387.
[9] G. Padmavathi, K. K. Chaudhuri,, D. Rajeshwer, G. Sreenivasa Rao, K.R. Krishnamurthy, P.C. Trivedi, K. K. Hathi, N. Subramanyam, Kinetics of n-dodecane dehydrogenation on promoted platinum catalyst, Chemical Engineering Science 60 (2005) 4119-4129.
[10] M. M. Bhasin, J.H. McCain, B.V. Vora, T. Imai, P.R. Pujado, Dehydrogenation and oxydehydrogenation of paraffins to olefins, Applied Catalysis A: General 221 (2001) 397-419.
[11] Joseph A. Kocal, Bipin V. Vora, Tamotsu Imai, Production of linear alkylbenzenes, Applied Catalysis A: General 221 (2001) 295-301.
[12] S. D. Harris, L. Elliott, D. B. Ingham, M. Pourkashanian, C. W. Wilson, The optimisation of reaction rate parameters for chemical kinetic modelling of combustion using genetic algorithms, Computer Methods in Applied Mechanics and Engineering 190 (2000) 1065-1090
[13] André Bardow, Wolfgang Marquardt, Incremental and simultaneous identification of reaction kinetics: methods and comparison, Chemical Engineering Science 59 (2004) 2673-2684
[14] G. S. G. Beveridge, R. S. Schechter, Optimization: Theory and Practice, New York: McGraw-Hill, 1970.
[15] H. Rabitz, M. Kramer, D. Dacol, Sensitivity Analysis in Chemical Kinetics, Annual Review of Physical Chemistry 34 (1983) 419-461.
[16] Herschel Rabitz, Chemical sensitivity analysis theory with applications to molecular dynamics and kinetics, Computers & Chemistry 5 (1981) 167-180.
[17] Robert Michael Lewis, Virginia Torczon, Michael W. Trosset, Direct search methods: then and now, Journal of Computational and Applied Mathematics 124 (2000) 191-207.
[18] Erwie Zahara, Yi-Tung Kao, Hybrid Nelder-Mead simplex search and particle swarm optimization for constrained engineering design problems, Expert Systems with Applications 36 (2009) 3880-3886.
[19] Rachid Chelouah, Patrick Siarry, Genetic and Nelder-Mead algorithms hybridized for a more accurate global optimization of continuous multiminima functions, European Journal of Operational Research 148 (2003) 335-348.
[20] C. J. Price, I. D. Coope, D. Byatt, A Convergent Variant of the Nelder–Mead Algorithm, Journal of optimization theory and applications 113 (2002) 5-19.
[21] R. Nakamura, M. Shimoji, H. Niiyama, Strategies for using a computer-operated reaction system for the evaluation of catalyst activity by optimization of product yield, Catalysis Today 10 (1991) 119-129.
[22] Jeffrey C. Lagarias, James A. Reeds, Margaret H. Wright, Paul E. Wright, Convergence properties of the Nelder-Mead simplex method in low dimensions, SIAM Journal of Optimization 9 (1998) 112-147.
[23] Marco A. Luersen, Rodolphe Le Riche, Globalized Nelder–Mead method for engineering optimization, Computers and Structures 82 (2004) 2251-2260.
[24] Julian Martinez, J.M. Martinez, Fitting the Sovova's supercritical fluid extraction model by means of a global optimization tool, Computers and Chemical Engineering 32 (2008) 1735–1745.
[25] Maryam Mohagheghi, Gholamreza Bakeri, Maryam Saeedizad, Study of the Effects of External and Internal Diffusion on the Propane Dehydrogenation Reaction over Pt-Sn/Al2O3 Catalyst, Chemical Engineering & Technology 30 (2007) 1721-1725.
[26] R.B. Bird, W.E. Stewart, E.N. Lightfoot, Transport Phenomena, second edition, John Wily, New York, 2002.
[27] N. George, B.V. Kamath, A.G. Basrur, K.R. Krishnamurthy, Lithium Promoted Pt-Sn/Al2O3 catalysts for dehydrogenation of n-decane: Influence of Lithium metal precursors, Reaction Kinetics and Catalysis Letters 59 (1996) 315-323.
[28] Jose O. Valderrama, The State of the Cubic Equations of State, Industrial & Engineering Chemistry Research 42 (2003) 1603-1618.
[29] G. Zahedi, H. Yaqubi, M. Ba-Shammakh, Dynamic modeling and simulation of heavy paraffin dehydrogenation reactor for selective olefin production in linear alkyl benzene production plant, Applied Catalysis A: General 358 (2009) 1-6.
[30] Curtis F. Gerald, Patrick O. Wheatley, Applied Numerical Analysis, 6th Edition, Addison Wesley, 1999.